ISBN: 978-3-95450-222-6 ISSN: 2673-5350 doi:10.18429/JACoW-IBIC2020-TUPP09

MULTIPLEXER SYSTEM FOR THE SPEAR3 BOOSTER BPM UPGRADE*

F. Toufexis†, L. Campana‡, P. Boussina, J.J. Sebek, J. Corbett, SLAC, Menlo Park, CA 94025, USA

Abstract

BPM measurements in booster synchrotrons are often only critical during accelerator commissioning or when a problem occurs. As a result, many facilities do not make large investments in booster BPM signal processors; they either have very few BPMs and/or use older generation processors. The SPEAR3 booster BPM processor system, for instance, has operated since 1990 with commercial multiplexers to switch between BPM button signals into a single dated analog BPM processor that was developed at SLAC. This system has reached its end-of-life so we are in the process of upgrading to modern multiplexers that feed a pair of turn-by-turn Libera SPARK-ERXR processors. This low-cost solution gives us the ability to arbitrarily multiplex between BPM signals during the energy ramp with modern BPM processors. The system can either measure 2 BPMs turn-by-turn in parallel during the entire energy ramp, or sequentially measure all BPMs (2 at a time) at different time slices within the ramp. Here we show measurements of the MiniCircuits switch we chose as well as our architecture for the upgrade.

INTRODUCTION

The SPEAR3 injector was commissioned in 1990 [1], and includes a 120 MeV linac injector with a thermionic RF gun [2], the booster synchrotron [3] and the Transport Lines. The entire injector, including the Transport Lines, is equipped with stripline-style Beam Position Monitors (BPMs). The original booster synchrotron BPM electronics used a commercial multiplexer to switch between BPM button signals into an in-house built analog BPM processor [4]. Out of the 40 booster BPMs, 20 are connected to long-haul cables that come out of the ring and are connected to the legacy BPM processor system. In this system, the 20 BPMs are connected to three slow multiplexer modules (referred to as the R10Ts). The output of these three multiplexers is connected to a faster multiplexer. The output of this multiplexer is filtered and then connected to an in-house BPM processor. Two different software systems can obtain the orbit from the booster: one system can get the average position in a number of time slots per booster ramp for one BPM, while the other system can get the position in several time slots for all BPMs in the same ramp.

At the time of this writing two (plus a spare) Instrumentation Technologies Libera SPARK-ERXR Turn-by-Turn (TbT) BPM processors have been installed at the booster and have gone through preliminary testing. We are also building two new multiplexer chassis that will connect the 20 connected booster BPMs into the SPARK processors to measure the orbit on a TbT basis during a booster ramp. We have investigated commercial switch options to replace the R10Ts; there are several option with sub-microsecond switching time but cost upwards of $7,000 for a 10-input switch that is not financially attractive. The Mini-Circuits USB-1SP16T-83H was the lowest cost option we found, had adequate specifications for our needs, and was readily available to purchase. The specifications are summarized in Table 1.

This work is organized as follows: we begin with time-domain and frequency domain measurements of the switch in the lab. Then we show measurements with the actual BPM signals from the booster. Finally we show the overall architecture of the new system we are building.

TIME-DOMAIN LAB MEASUREMENTS

The MiniCircuits switch provides both a TTL and USB interface. The USB interface can be used for slow switching on the order of milliseconds according to the manual; therefore we use the TTL interface. The unit has a DB9 connector to provide power and TTL signals if USB is not being used. We made a custom cable; one end had a DB9 connector, and the other had two banana plugs to connect ground and power as well as 5 coaxial cables with BNC connectors to connect the TTL signals to a delay generator for testing. The measurement setup is shown in Figure 1.

First we tested with one RF input signal at 400 MHz and −10 dBm. We programmed the delay generator to toggle 1 channel as shown in Figure 2a, switching between the signal and an unconnected input. We noticed that the gating on/off of the output signal jittered with respect to the signal generator. We subsequently connected a second RF input signal, now switching between two inputs. Figure 2b shows the transition of the output. The whole transition itself takes less than 5 µs as specified; however, the transition time with respect to the delay generator signal again showed jitter of about 10 µs. We suspect this is due to the microprocessor on the switch that internally controls the switching; most likely the microprocessor periodically checks the input TTL

Table 1: Mini-Circuits USB-1SP16T-83H Switch Specs

Frequency	1 MHz – 8 GHz
Isolation	63 dB Min (0 GHz – 3 GHz)
Transition Time	5 µs
Power Handling	30 dBm
Insertion Loss	7.5 dB Max (0 GHz – 3 GHz)
Interface	USB & TTL
Inputs	16
Price	$1,835

* Work sponsored by US Department of Energy Contract DE-AC02-76SF00515.
† ftouf@slac.stanford.edu
‡ Currently at Dipartimento di fisica, Sapienza università di Roma, Rome, Italy

ISBN: 978-3-95450-222-6 ISSN: 2673-5350 doi:10.18429/JACoW-IBIC2020-TUPP09

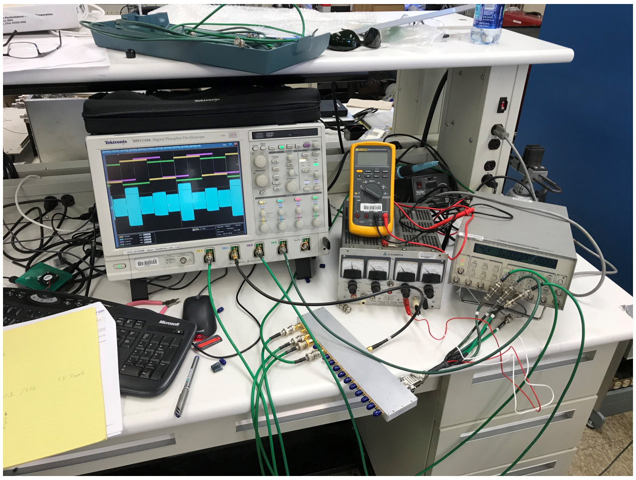

Figure 1: Measurement setup. The scope shows the continuous switching between 4 channels of different frequency and amplitude.

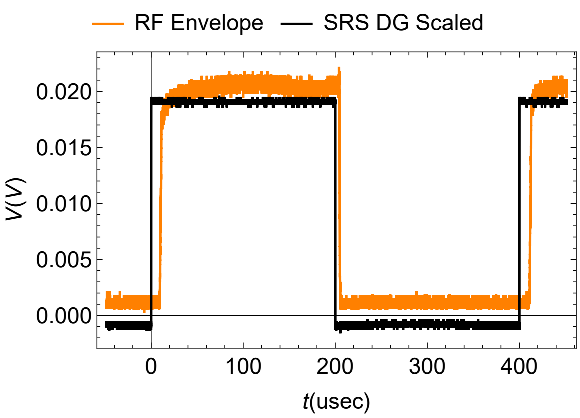

(a) On/off characteristics

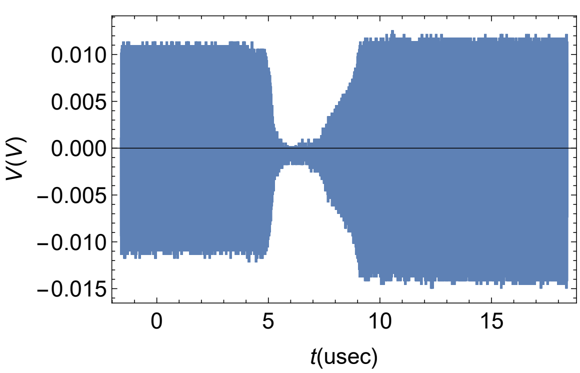

(b) Switching between two RF input signals.

Figure 2: Transition data.

signals and decides how to modify the switch configuration. Therefore we consider the effective dead time of a transition to be 20 µs.

Finally, we tested a configuration with continuous switching between four channels. We programmed the delay generator to toggle 3 control TTL signals in a pattern that would cause the switch to alternate between 4 channels. We connected signals with frequencies between 250 MHz and 500 MHz, and power between −20 dBm and −10 dBm. The resulting output signal is shown in Figure 1. As expected, the switching characteristics appeared the same as in the two-channel case.

VNA MEASUREMENTS

We next connected port 1 of a Vector Network Analyzer (VNA) to channel 1 of the switch and port 2 to the COM port. Without changing this setup, we measured S-parameters for 3 cases: a) channel 1 enabled, b) channel 2 enabled, and c) channel 16 enabled. The different channels were enabled through EPICS using a prototype controller based on a Raspberry Pi and an Arduino.

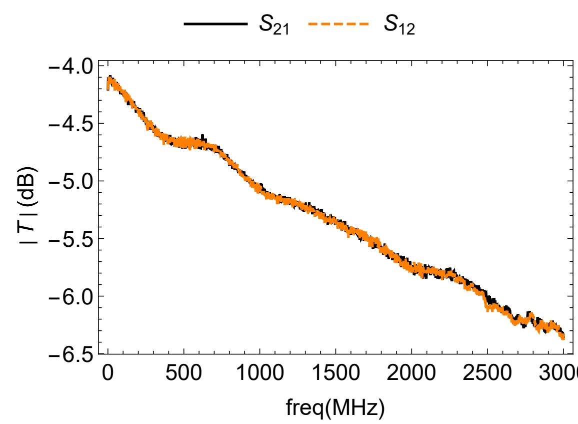

(a) Attenuation through the switch.

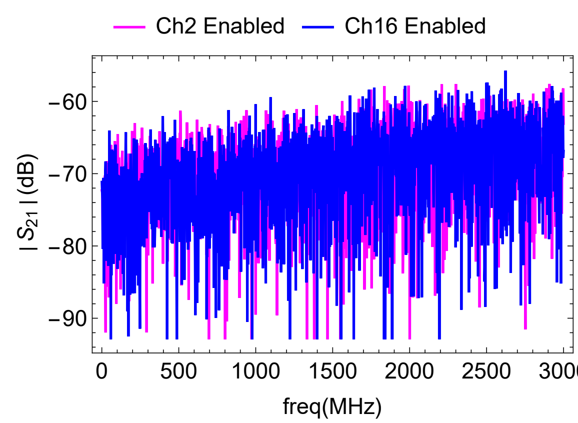

(b) Isolation when a different channel is enabled.

Figure 3: Attenuation and isolation data.

Figure 3a shows the transmission from channel 1 to the COM port and reverse when channel 1 is activated. The switch is near perfectly reciprocal. Attenuation increases almost linearly with increased frequency from about 4.2 dB at near DC frequencies to about 6.4 dB at 3 GHz. This is a much improved response when compared to the existing system. Figure 3b shows the isolation from channel 1 to the COM port when a different channel is enabled. The switch has around 60 dB isolation.

ISBN: 978-3-95450-222-6 ISSN: 2673-5350 doi:10.18429/JACoW-IBIC2020-TUPP09

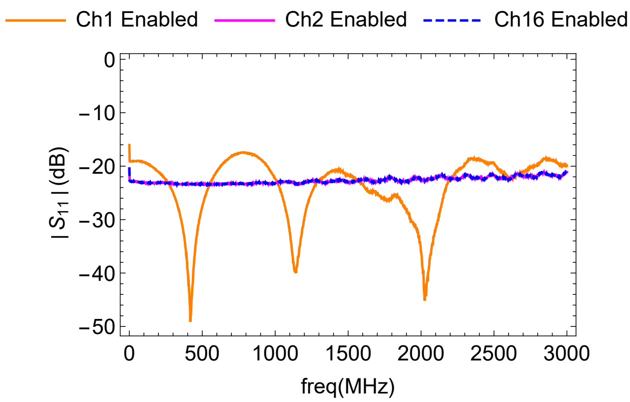

(a) Reflection from channel 1.

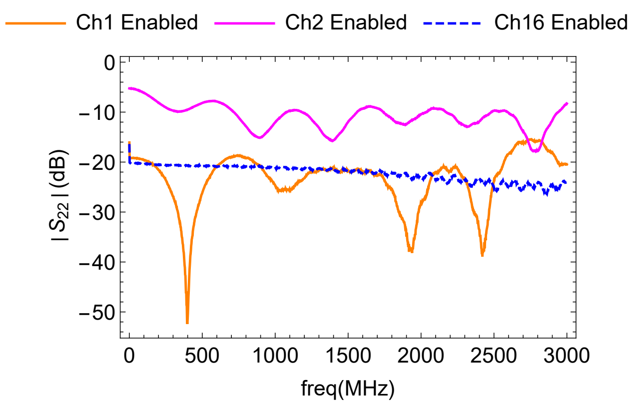

(b) Reflection from the COM port.

Figure 4: Reflection data.

Figure 4 shows the reflection from channel 1 and the COM port for different enabled channels. The input is always well-matched irrespective of the enabled channel. The output is not always well-matched; we are not sure why, but we do not expect it to be an issue as the output of the switch will be connected to a BPM processor that is not generating signals.

BEAM-BASED MEASUREMENTS

We further performed a number of measurements with the booster beam and the actual BPM signals to see how the switch affects the waveforms. Figure 5 shows a single-pass BPM waveform directly on the scope and through the switch. As expected from the attenuation of the switch, the amplitude is roughly half. We see an additional reduction at the positive part of the waveform, but overall the switch does not appear to substantially degrade the waveform.

We then connected one BPM button signal on channel 1 and set the switch on that channel. Figure 6 shows the BPM waveform through the switch for multiple turns while channel 1 was activated. We can observe oscillations on the envelope. We further connected a second BPM to channel 2 through a 6 dB attenuator and set the switch to alternate between channel 1 and 2. Figure 7 shows the transition from channel 2 to channel 1. From this data we believe that we can post-process the BPM data by identifying transitions

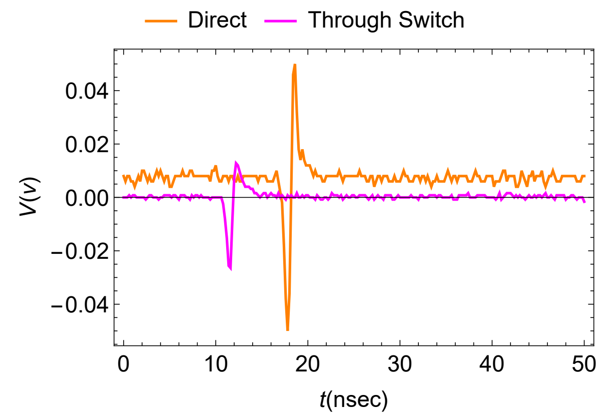

Figure 5: Direct BPM waveform and through the switch.

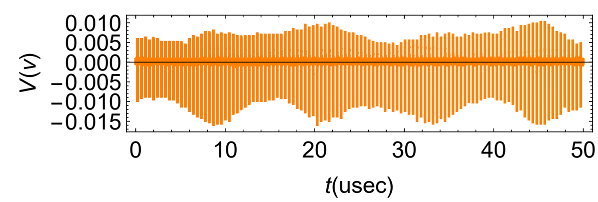

Figure 6: BPM waveform of several turns through the switch.

from the signal amplitude in software. Once we identify transitions, since we know the transition time and sequence, we can discard the data points close to the transitions.

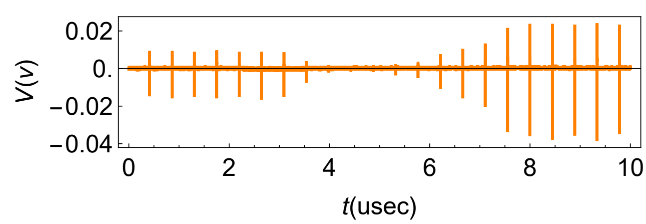

Figure 7: BPM waveform during a transition between two channels.

BPM SWITCH ARCHITECTURE & PROTOTYPE

Figure 8a shows an overview of the BPM multiplexer system. The inputs of four MiniCircuits switches are connected to the ABCD buttons coming from the synchrotron. The outputs are connected to the inputs of one SPARK-ERXR module. The switches are controlled through the DB9 TTL interface. A microcontroller Printed Circuit Board (PCB) is used to control the four switches. We have chosen the Infineon XMC4800 microcontroller since it is an industrial part with long support lifetime and has a simple software environment to configure its peripherals and program it, and can receive commands through a USB serial interface. An EPICS IOC can then send commands to the microcontroller using EPICS `SteamDevice`. The microcontroller can be directly connected on the USB port of a computer (such as a RaspberryPi) that hosts the IOC. Alternatively, the microcontroller can be connected to a terminal server; the IOC

ISBN: 978-3-95450-222-6 ISSN: 2673-5350 doi:10.18429/JACoW-IBIC2020-TUPP09

will reside on a server and send commands over the network. The 10 Hz injector trigger is also supplied to the microcontroller. We developed a proof-of-concept prototype shown in Fig. 8b. In the protype we used the XMC4700 development board connected to a vector board with DB9 connectors for the switches and BNC trigger input. The microcontroller is connected to the USB port of a Raspberry Pi that hosts an EPICS IOC.

This system can operate in two modes: a) static, and b) alternating. In the static mode the switches are set to one BPM and the SPARK reads only this BPM. In the alternating mode the microcontroller cycles through the connected BPMs constantly through the booster ramp. In this case the SPARK reads positions from a number of time slices from all the connected BPMs during the booster ramp. The 10 Hz injection trigger is used to signal the beginning of booster ramp. A software script then postprocesses the SPARK data and assigns different portion of the TbT data to different BPMs; the switch between BPMs can be identified by looking when the sum signal falls bellow a certain threshold. Additionally we can connect one of the switch inputs to the RF signal of the booster to act a fiducial.

Figure 9 shows measured data from the SPARK while switching between four BPMs. In the x position we can see jumps in the data points around the BPM transitions. However, in the same transitions we can see the sum signal becomes low as expected from the switch characteristics. We can identify the transition times using the sum information and then discard the data points around the switch transitions.

We are building two multiplexer chassis with the Mini-Circuits switch in order to connect the 20 booster BPMs to the two SPARK-ERXR TbT Processors. Each chassis will have internally 4 switches for the 4 BPM buttons. The booster ramp is approximately 30 ms. If we have 10 BPMs connected to each chassis, then we can measure each BPM for 3 ms during the ramp. If we further split this in 30 time slices, then a time slice for one BPM is 100 µs. Subtracting the 20 µs of dead time during a BPM switch, we can sample 80 µs or approximately 150 turns per BPM per time slice.

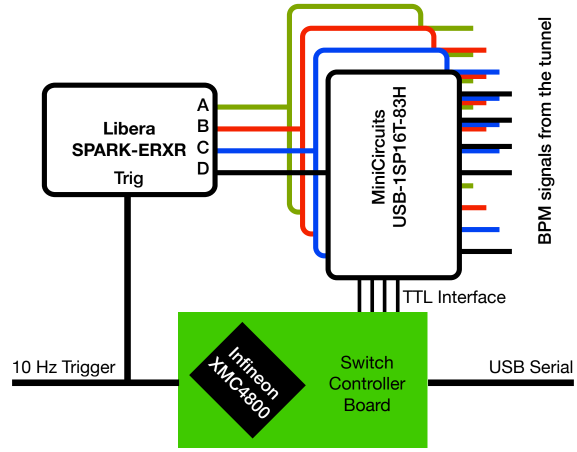

(a) Schematic of the proposed system upgrade.

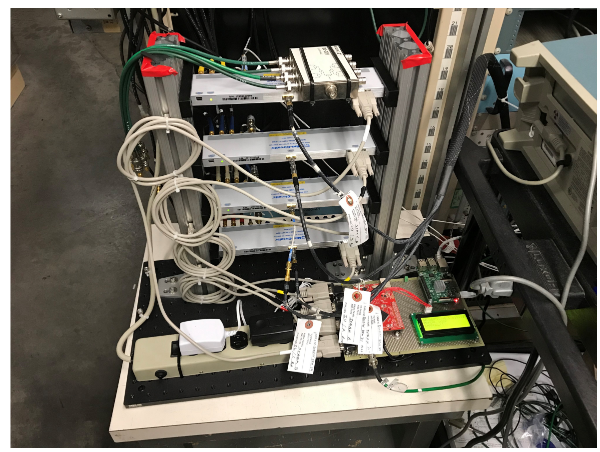

(b) Picture of the proof-of-concept prototype.

Figure 8: BPM multiplexer system.

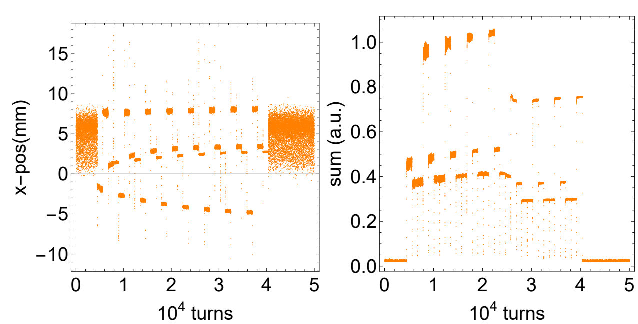

Figure 9: Measured data from the SPARK while switching between four BPMs.

SUMMARY

In this work we showed proof-of-concept measurements for a low-cost BPM multiplexer system for the SPEAR3 booster synchrotron. Instead of having one BPM processor per physical BPM we will use a set of commercial multiplexers that feed two Libera SPARK-ERXR TbT BPM processors. The existing system also used multiplexers but has reached its end of life. We have evaluated a commercial switch and showed testing results both in the lab and with the actual BPM signals from the booster. From the data we collected, the unit has an average dead time due to switching of about 20 µs. The performance of this switch is adequate for the replacing the R10Ts in the booster BPM system. Finally we described the architecture for the upgrade. The system can either measure 2 BPMs TbT during the entire energy ramp, or sequentially measure all BPMs (2 at a time) at different time slices within the ramp.

ACKNOWLEDGMENTS

The authors would like to thank Shantha Condamoor, Scott Wallters, Kevin Helms, and the SPEAR3 operations staff for technical assistance.

ISBN: 978-3-95450-222-6 ISSN: 2673-5350 doi:10.18429/JACoW-IBIC2020-TUPP09

REFERENCES

[1] S. Baird and J. Safranek, "Commissioning the SSRL injector," in *Conference Record of the 1991 IEEE Particle Accelerator Conference*, vol. 5, May 1991, pp. 2865–2867. doi: 10.1109/PAC.1991.165129.

[2] M. Borland, "A High Brightness Thermionic Microwave Electron Gun," Ph.D. dissertation, Stanford University, Feb. 1991.

[3] H. Weidemann, M. Baltay, J. Voss, K. Zuo, C. Chavis, R. Hettel, J. Sebek, H. D. Nuhn, J. Safranek, L. Emery, M. Horton, J. Weaver, J. Haydon, T. Hostetler, R. Ortiz, M. Borland, S. Baird, W. Lavender, P. Kung, J. Mello, W. Li, H. Morales, L. Baritchi, P. Golceff, T. Sanchez, R. Boyce, J. Cerino, D. Mostowfi, D. F. Wang, D. Baritchi, G. Johnson, C. Wermelskirchen, B. Youngman, C. Jach, J. Yang, and R. Yotam, "The 3 GeV synchrotron injector for SPEAR," in *Conference Record of the 1991 IEEE Particle Accelerator Conference*, vol. 5, May 1991, pp. 2688–2690. doi: 10.1109/PAC.1991.165072.

[4] W. Lavender, S. Baird, S. Brennan, M. Borland, R. Hettel, H. D. Nuhn, R. Ortiz, J. Safranek, J. Sebek, C. Wermelskirchen, and J. Yang, "The SSRL injector beam position monitoring systems," in *Conference Record of the 1991 IEEE Particle Accelerator Conference*, vol. 2, May 1991, pp. 1151–1153. doi: 10.1109/PAC.1991.164563.